https://doi.org/10.5194/egusphere-2024-667
Preprint. Discussion started: 7 March 2024

Downward Coupling of Sudden Stratospheric Warmings: Important Role of Synoptic-Scale Waves Demonstrated by ERA5 Reanalysis

Tabea Rahm[1], Robin Pilch Kedzierski[2,1], Martje Hänsch[1], and Katja Matthes[1]

[1]GEOMAR Helmholtz Centre for Ocean Research, Kiel, Germany
[2]Meteorological Institute, Universität Hamburg, Hamburg, Germany

Correspondence: Tabea Rahm (trahm@geomar.de)

Abstract. Circulation anomalies accompanying Sudden Stratospheric Warmings (SSWs) can have a significant impact on the troposphere. This surface response is observed for some but not all SSWs, and their downward coupling is not fully understood. We use an existing classification method to separate downward- and non-propagating SSWs (d/nSSWs) in ERA5 reanalysis data for the years 1979–2019. The differences in SSW downward propagation in composites of spatial patterns clearly show that dSSWs dominate the surface regional impacts following SSWs. During dSSWs, the upper-tropospheric jet stream is significantly displaced equatorward. Wave activity analysis shows remarkable differences between d/nSSWs for planetary and synoptic-scale waves. Enhanced stratospheric planetary eddy kinetic energy (EKE) and heat fluxes around the central date of dSSWs are followed by increased synoptic-scale wave activity and even surface coupling for synoptic-scale EKE. An observed significant reduction in upper-tropospheric synoptic-scale momentum fluxes following dSSWs confirms the important role of tropospheric eddy feedbacks for coupling to the surface. Our findings emphasize the role of the lower stratosphere and synoptic-scale waves in coupling the SSW signal to the surface and agree with mechanisms suggested in earlier modeling studies.

1 Introduction

Sudden Stratospheric Warmings (SSWs) are characterized by an abrupt disruption of the stratospheric polar vortex during wintertime, along with a sudden increase in polar stratospheric temperatures of up to 50 K in a few days, which is induced by planetary waves propagating from the troposphere to the stratosphere (Scherhag, 1952; Labitzke and van Loon, 1999; Baldwin et al., 2021). In addition to vigorously affecting the stratosphere, an anomalously weak polar vortex, as observed during SSWs, is often followed by an equatorward shift of the tropospheric jet accompanied by cold-air outbreaks over North America and northern Eurasia as well as surface pressure anomalies resembling the negative phase of the Northern Annular Mode (NAM). As this tropospheric response can last for up to two months (Baldwin and Dunkerton, 2001; Thompson et al., 2002; Sigmond et al., 2013), these stratospheric events provide an important source of predictability for tropospheric weather (Kolstad et al., 2010; Tripathi et al., 2015; Scaife et al., 2016; Domeisen et al., 2020).

Different mechanisms have been suggested for stratosphere–troposphere coupling with the 'downward control' (Haynes et al., 1991) principle being one of the most renowned. This principle is derived from geostrophic, hydrostatic, and thermal

https://doi.org/10.5194/egusphere-2024-667
Preprint. Discussion started: 7 March 2024

wind balance, stating that flow perturbations imply a non-local response. Shaw et al. (2010) and Kodera et al. (2016) suggested the absorption and reflection of planetary waves as a possible mechanism. Another accepted mechanism for this coupling of the stratosphere to the troposphere is the eddy-zonal flow feedback, as described by Lorenz and Hartmann (2003). According to this positive feedback mechanism, baroclinic eddies in the form of synoptic-scale waves act to reinforce zonal mean stratospheric circulation anomalies.

However, the described long-lasting changes in the tropospheric state are not observed during every SSW. Several studies have investigated the factors that might influence the downward propagation of circulation anomalies. Kodera et al. (2016) investigated the downward influence of absorbing and reflecting SSWs, while Lehtonen and Karpechko (2016) and Hall et al. (2021) focused on the separation into split and displacement events. Nakagawa and Yamazaki (2006) as well as Bancalá et al. (2012), Barriopedro and Calvo (2014), and White et al. (2019) examined wave activity prior to SSWs onset. The results of these studies regarding the downward propagation of circulation anomalies and the surface impact associated with SSWs were, however, often inconsistent with previous results and strongly dependent on the classification algorithm (Maycock and Hitchcock, 2015; Lehtonen and Karpechko, 2016).

Karpechko et al. (2017) successfully separated SSWs according to their downward effects. Their study showed that SSWs followed by long-lasting tropospheric circulation anomalies (called downward-propagating SSWs: dSSWs) are characterized by a negative NAM index in the lower stratosphere and enhanced upward planetary wave propagation from the troposphere into the stratosphere during the first few days after their onset. These features are not observed during SSWs that do not show a strong and prolonged impact on the troposphere (non-propagating SSWs: nSSWs). Our study aims to complement the work of Karpechko et al. (2017) on the zonal mean by examining the differences in the spatial structures associated with dSSWs and nSSWs as well as changes in the position of the upper-tropospheric jet, as presented in Section 3.

Additionally, we perform a wave analysis separating planetary and synoptic-scale waves. A recent study by Pilch Kedzierski et al. (2020) observed increased vertical propagation of wave numbers 4 to 6 to the stratosphere, especially during SSWs. Modeling studies by Domeisen et al. (2013) as well as Garfinkel et al. (2013), Kunz and Greatbatch (2013), Hitchcock and Simpson (2014), and Smith and Scott (2016) highlighted the importance of the synoptic eddy feedback for the tropospheric response to SSWs. Observationally, a role for synoptic-scale waves in stratosphere-troposphere coupling was also pointed out by Limpasuvan et al. (2004), who considered all SSWs, regardless of surface impacts. Our study adds to these previous findings by yielding an observational confirmation of the modeling results for planetary and synoptic-scale wave activity during SSWs and connecting them to the classification based on the tropospheric impact into d/nSSWs. By combining these two approaches, we highlight the role of both planetary and synoptic-scale waves for the downward propagation of the SSW signal and, in addition, help disentangle their complex interplay during the different d/nSSW stages, as discussed in Section 4.

https://doi.org/10.5194/egusphere-2024-667
Preprint. Discussion started: 7 March 2024

2 Data and Methods

2.1 Data

This study uses the new ERA5 reanalysis data set of the European Centre for Medium-Range Weather Forecasts (ECMWF) (Hersbach et al., 2020). The data covering the period from January 1979 to February 2019 include temperature, geopotential, and zonal and meridional wind and have a 6-hourly temporal resolution. They are interpolated on an even spatial grid with a horizontal resolution of 2.5° longitude x 2.5° latitude and 37 pressure levels between 1000 hPa and 1 hPa. Two additional variables that are used are 2-meter temperature and mean sea level pressure (MSLP). Daily mean values are calculated prior to the subsequent analysis. The geopotential is converted to geopotential height by division by the standard acceleration due to gravity.

2.2 Methods

The algorithm used to identify SSWs was applied to daily reanalysis data and follows the method used by Karpechko et al. (2017), which is based on the World Meteorological Organization (WMO) criteria: A Sudden Stratospheric Warming is identified when the zonal mean zonal wind at 60° N on the 10 hPa level is reversing from westerly to easterly winds during the wintertime throughout November to March (NDJFM) indicating a breakdown of the polar vortex with the central date as the first day of reversed winds (Charlton and Polvani, 2007).

A simple proxy of the NAM index is derived as the (cosine-latitude) area-weighted mean of polar cap geopotential height anomalies normalized by the standard deviation on each pressure level, with inverted sign (Baldwin and Thompson, 2009; Karpechko et al., 2017). We then use the NAM index to categorize SSWs according to whether the signal propagates to the troposphere into dSSWs and nSSWs by analyzing the persistence of the NAM index near the surface and in the lowermost stratosphere: a dSSW is identified when the mean NAM index for the period from day 8 to 52 after the central date at the 1000 hPa level is negative with at least 50 % of the days showing a negative value at 1000 hPa and at least 70 % of the days showing a negative value at the 150 hPa level. If these three criteria are not met, the event is classified as nSSW (Karpechko et al., 2017).

As the upper-tropospheric jet stream is a driving element of mid-latitude weather, we include a comparison of the temporal evolution of jet latitude around the central date of d/nSSWs. To calculate upper-tropospheric jet latitude, we adapt the approach by Archer and Caldeira (2008) for grid points north of 30° N:

$$L_i^{NH} = \frac{\sum_{j=30N}^{j=90N} \left[\sum_{k=400hPa}^{k=100hPa} \left(m_k \times \sqrt{u_{i,j,k}^2 + v_{i,j,k}^2} \right) \right] \times \varphi_{i,j}}{\sum_{j=30N}^{j=90N} \sum_{k=400hPa}^{k=100hPa} m_k \times \sqrt{u_{i,j,k}^2 + v_{i,j,k}^2}} \quad (1)$$

Here m_k applies area-weighting and we also multiply by the cosine of latitude to account for differences in grid cell area.

A fast Fourier transform (FFT) in longitude is used to get temperature (T') and wind (u', v') anomalies from the zonal mean, extracting the anomalies of planetary-scale wave numbers 1 to 3 and synoptic-scale wave numbers in the range 4 to 15, a range typically used for the study of Rossby wave packets (Wolf and Wirth, 2015; Fragkoulidis et al., 2018). To investigate the effect

https://doi.org/10.5194/egusphere-2024-667
Preprint. Discussion started: 7 March 2024

of planetary and synoptic-scale wave activity on the downward propagation of the SSW signal, eddy kinetic energy (EKE) as well as eddy heat and momentum fluxes ($\overline{v'T'}$ and $\overline{u'v'}$, respectively) are calculated using the planetary (wave numbers 1–3) and synoptic-scale (wave numbers 4–15) components filtered from the temperature and wind anomalies. Pressure-weighting is applied to improve the detectability of anomalies around and below the tropopause level.

Composites over all dSSW and nSSW events in the period covered by the ERA5 data set are evaluated using Welch's t-test with a 95 % (90 %) level of confidence to identify locations with significant differences from climatology.

3 Downward Propagation Patterns of SSWs

3.1 Zonal Mean

To ensure accordance with the results from Karpechko et al. (2017), we start by reproducing their results using an updated ERA5 data set, which yields two additional SSWs (12.02.2018 and 01.01.2019) for the period 1979–2019. Out of the 25 SSWs identified during this period, 14 (56 %) were categorized as dSSWs and 11 (44 %) as nSSWs (see Table S1 in supplement). Following Karpechko et al. (2017), the event on the 24th of March 2010 is excluded to prevent a composite overlap with the aftermath of the SSW event on the 9th of February 2010. The dates of the SSWs, their categorization, and the ratio of dSSWs to nSSWs agree well with the results obtained by Karpechko et al. (2017) using ERA-Interim reanalysis data.

Figure S1 in the supplement shows time-height composites of the NAM index for all SSWs, dSSWs, and nSSWs, following Karpechko et al. (2017). The observed pattern is almost identical to their Fig. 1. Anomalies during dSSWs are in general stronger and longer-lasting than during nSSWs. Especially the lower stratosphere shows persistent negative NAM values during dSSWs, which are not observed during nSSWs. Once the results by Karpechko et al. (2017) are reproduced using the new ERA5 reanalysis data set with two additional SSWs, we proceed to examine the spatial patterns of circulation anomalies accompanying dSSWs and nSSWs.

3.2 Spatial Downward Propagation Patterns

For convenience, we will describe the spatial patterns of d/nSSW anomalies following the typical evolution of SSW signals: starting in the stratosphere and propagating down to the surface. SSW precursors will be discussed separately afterwards.

Temperature anomalies at different stratospheric levels during dSSWs and nSSWs are shown in Figs. 1a-c and 2a-c, respectively. Stratospheric geopotential height anomalies can be seen in Figs. 3a-c and 4a-c.

During dSSWs, positive anomalies of both temperature and geopotential height appear first in the stratosphere at upper pressure levels before they propagate downward to the lowermost stratosphere, where they persist at the 150 hPa level for the observed period of 45 days after the central date. These anomalies are already visible at the 10 hPa level before the central date with widespread positive temperature anomalies having their maximum over Northern Asia and positive geopotential height anomalies maximizing over the North Pacific. Both temperature and geopotential height anomalies have a very annular structure and reach the highest values in the middle stratosphere (10 and 50 hPa, see Figs. 1a-b and 3a-b) directly after the

https://doi.org/10.5194/egusphere-2024-667
Preprint. Discussion started: 7 March 2024

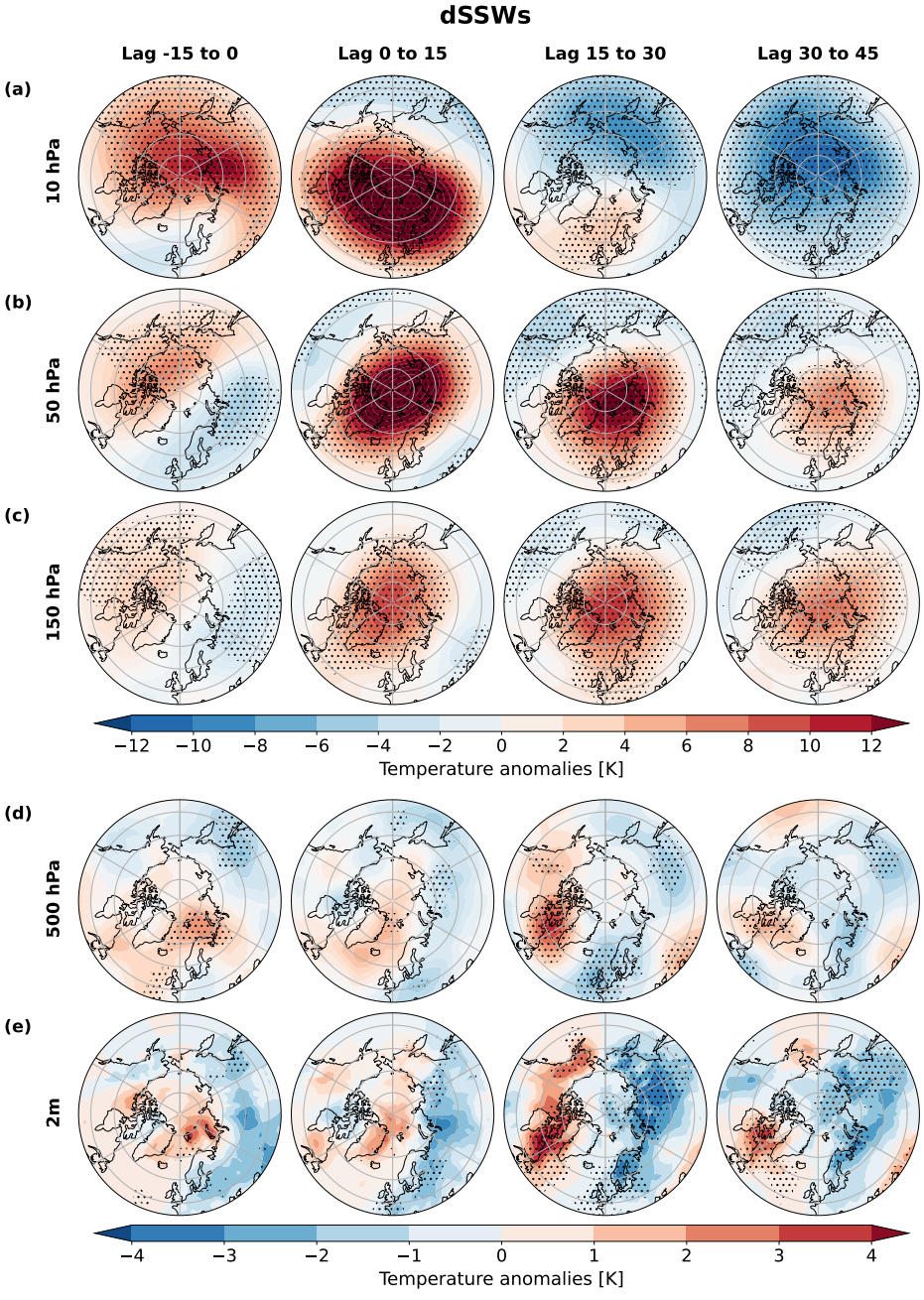

Figure 1. Composite of the temporal evolution of temperature anomalies averaged over 15-day periods around the central dates on different pressure levels during dSSWs. The hatching indicates regions where the composited anomalies are significantly different from climatology at a 95 % level.

https://doi.org/10.5194/egusphere-2024-667
Preprint. Discussion started: 7 March 2024

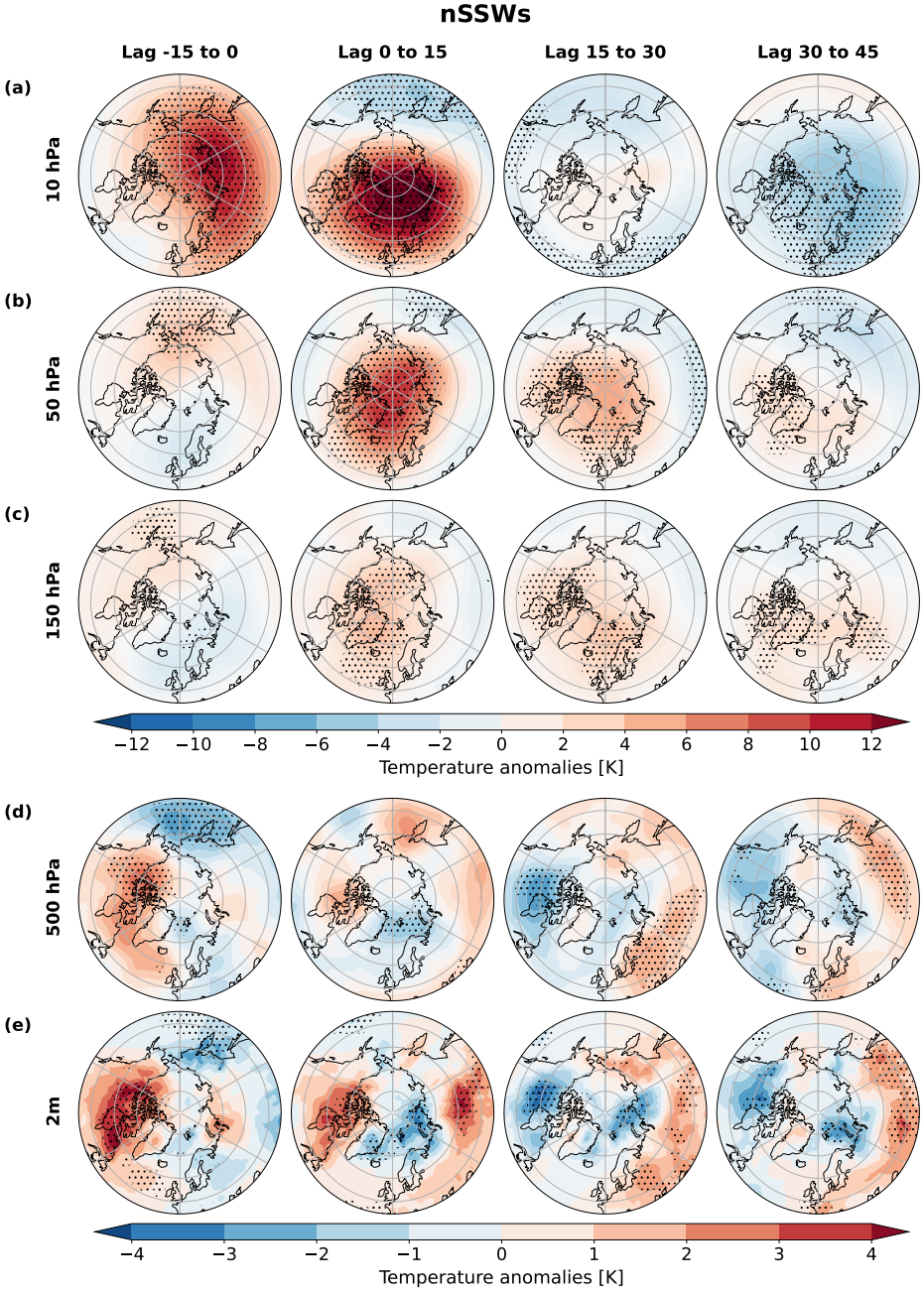

Figure 2. As Fig. 1 but for temperature anomalies during nSSWs. Again, hatching indicates significant differences at a 95 % level. Please note the different scale for the colorbar in d) and e).

https://doi.org/10.5194/egusphere-2024-667
Preprint. Discussion started: 7 March 2024

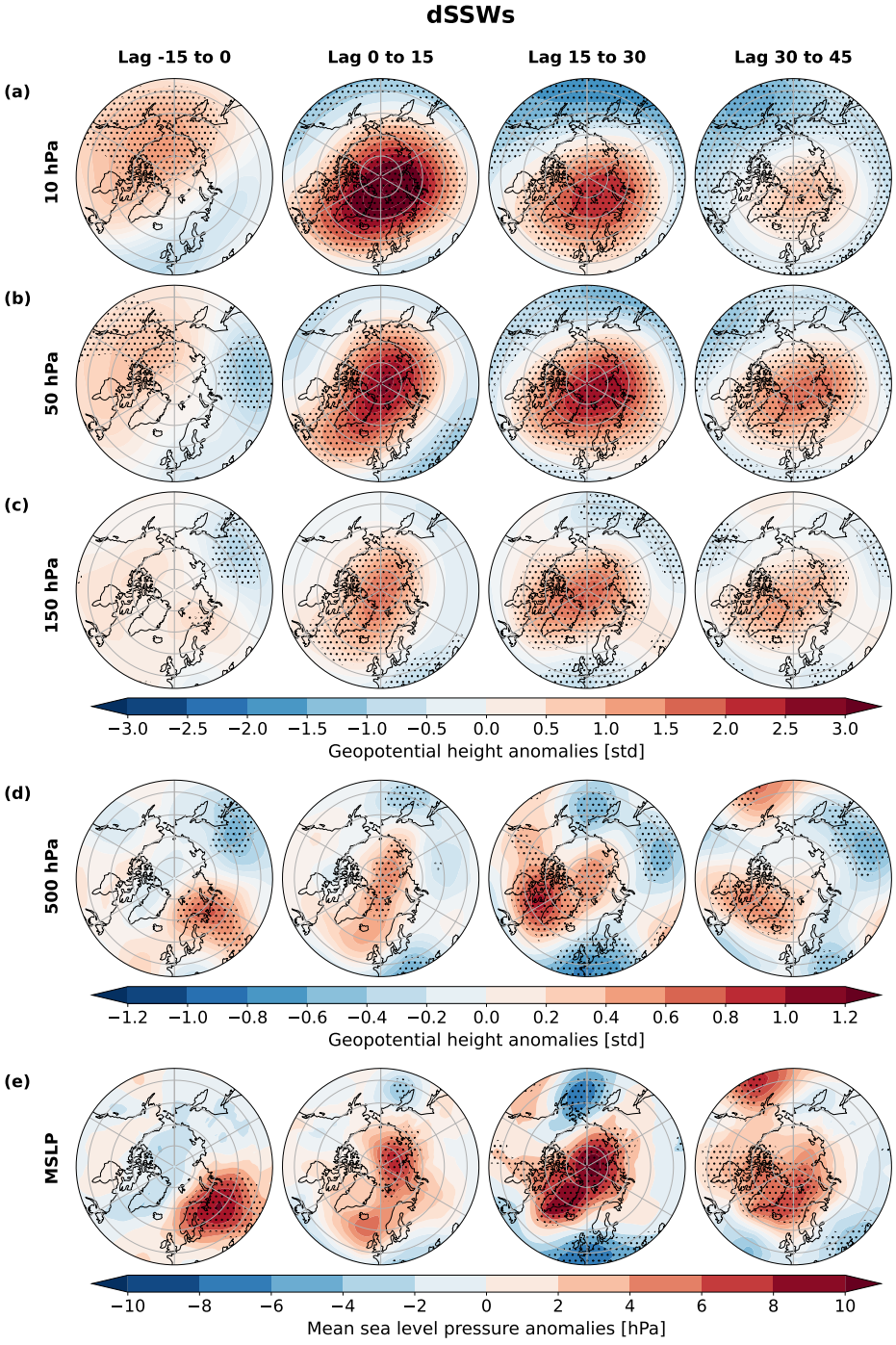

Figure 3. As Fig. 1 but for geopotential height and MSLP anomalies during dSSWs. Again, hatching indicates significant composited anomalies at a 95 % level. Please note the different scale for the colorbar in d) and the different unit in e) for the anomalies in MSLP.

https://doi.org/10.5194/egusphere-2024-667
Preprint. Discussion started: 7 March 2024

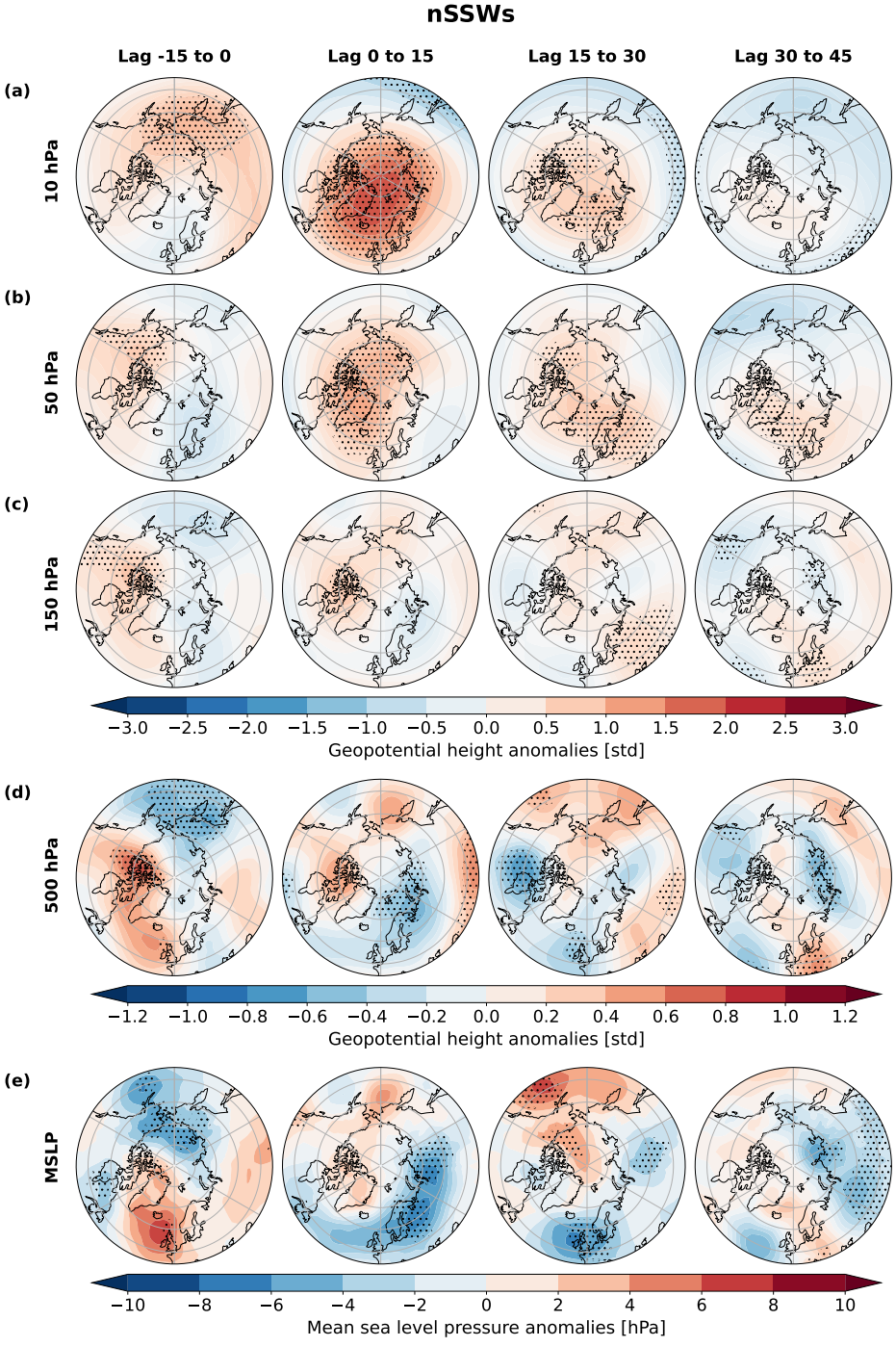

Figure 4. As Fig. 3 but for geopotential height and MSLP anomalies accompanying nSSWs.

https://doi.org/10.5194/egusphere-2024-667
Preprint. Discussion started: 7 March 2024

central date while the signal needs more time to propagate to the lowermost stratosphere (150 hPa, Figs. 1c and 3c), where the maximum anomalies are observed at lag 15 to 30.

Also during nSSWs (Figs. 2a-c and 4a-c), temperature and geopotential height anomalies appear first at the upper pressure levels before the central date. At the 10 hPa level, annular geopotential height and temperature anomalies similar to Figs. 1 and 3 can be seen. As during dSSWs, the strongest anomalies at the upper levels appear around the central date, but in contrast to the anomalies observed during dSSWs, they do not propagate downward to lower levels. Already at the 50 hPa level, only very weak temperature and geopotential height anomalies are observed and the amplitude decreases even more near the tropopause.

Overall, the stratospheric anomalies accompanying SSWs show an almost pure NAM signal indicating a very weak polar vortex. This negative NAM state is more pronounced and longer-lasting for dSSWs than for nSSWs, as also seen in Section 3.1 for the zonal mean, and followed by a stronger vortex recovery and colder stratosphere after dSSWs.

Temperature anomalies in the mid-troposphere and near the surface are shown for dSSWs and nSSWs in Figs. 1d-e and 2d-e, respectively. Figures 3d-e and 4d-e contain the composites for tropospheric geopotential height and MSLP anomalies during dSSWs and nSSWs. Note the different color scales and magnitude of the tropospheric anomalies compared to the stratospheric values for both temperature and geopotential height. Please also note that tropospheric anomalies before the central date are described separately in the next subsection.

In general, the tropospheric anomalies show more zonal structures, especially in the temperature anomalies. During dSSWs, the strongest tropospheric anomalies are observed after lag 15. These anomalies are characterized by above-average temperature over the western North Atlantic and eastern North America, cold anomalies over Northern Europe and most of Siberia as well as significantly enhanced geopotential height anomalies over the pole extending over the western North Atlantic region. This is the downward influence of dSSWs expected from the classification algorithm used, which was already found to be the dynamic response to reduced stratospheric jet speeds as during SSWs in earlier studies (Thompson et al., 2002; Hitchcock and Simpson, 2014; Kidston et al., 2015).

After the central date of nSSWs, from lag 15 to 30, the near-surface temperature anomalies show the opposite pattern compared to dSSWs. This period is characterized by positive temperature anomalies over most of Eurasia, whereas northernmost America experiences colder-than-average temperatures. In contrast to dSSWs, where the MSLP anomalies associated with the negative NAM phase propagate down to the troposphere, the surface after nSSWs does not show a clear NAM pattern but rather smaller-scale and weaker MSLP anomalies, in combination with weak geopotential height anomalies at the 500 hPa level.

Composites of d/nSSW differences in temperature and geopotential height anomalies can be found in the supplementary material in Figs. S2 and S3.

3.2.1 Tropospheric Precursors

Before dSSWs (Fig. 1d-e), temperature anomalies do not appear to have a distinct and significant structure as in the stratosphere. Instead, weak but significant warm anomalies appear over the Barents Sea and are possibly linked to changes in sea ice. Geopotential height before the central date of dSSWs (Fig. 3d-e) shows weak significant positive anomalies over the Ural

https://doi.org/10.5194/egusphere-2024-667
Preprint. Discussion started: 7 March 2024

region in the mid-troposphere (500 hPa) that amplify at the surface to a stronger and more extended signal in MSLP. This is in line with enhanced sea level pressure in this area found by Kretschmer et al. (2017) as a consistent precursor of weak polar vortex states and appears as a purely tropospheric feature before the onset of dSSWs.

For nSSWs (Fig. 2d-e), strong tropospheric temperature anomalies can be seen already before the onset. The 15 days before the central date of the nSSW composite are characterized by strong positive temperature anomalies up to 4 K over most of Canada and the Labrador Sea. Weak but statistically significant negative temperature anomalies dominate over the North Pacific, which are accompanied by negative geopotential height and MSLP anomalies near the Aleutian Low region (Fig. 4d-e). Over Canada, geopotential height anomalies before the onset of nSSWs show above average values at the 500 hPa level, which, interestingly, are not supported by the signal in MSLP.

Kretschmer et al. (2017) described a stationary high pressure system over the Ural mountains to be a consistent precursor of the most extremely weak vortex states in reanalysis data, which is in accordance with a weaker vortex state during and right after the breakup for dSSWs compared to nSSWs. White et al. (2019) identified a strengthening of the climatological Siberian high prior to the onset of dSSW events. Also, Peings (2019) found Ural blocking to be a potential precursor of early-winter stratospheric warmings in a high-top model, thereby further supporting the results shown here. Domeisen et al. (2020) found that European blocking conditions before SSWs can favor Greenland blocking conditions after SSWs. These results agree with our findings for dSSWs. The composites for dSSWs show an area of strong, statistically significant MSLP anomalies over eastern and northern Europe preceding SSWs, which are less pronounced at the 500 hPa level, and subsequently move westwards towards Greenland and the Labrador Sea at lags 15 and 30, while the positive anomalies near the Pole are established simultaneously.

The spatial patterns and especially the d/nSSW differences seen in the troposphere support the classification according to the downward propagation and highlight the importance of the lower stratosphere for the downward propagation of the stratospheric signal.

Interestingly, a recent study by Reichler and Jucker (2022) has explored a different perspective on strong stratospheric events. They have identified 'positive wave driving events' (PWDs) as periods when the accumulated upward wave activity flux in the lower stratosphere (i.e. the vertical component of the Eliassen-Palm flux at the 100 hPa level) exceeds an empirically determined threshold. The study's spatial patterns in the MSLP and 2m-temperature response (their Figs. 8 and A1) as well as its precursors for PWDs (their Fig. 4) show very similar features to our dSSW composites. A comparison of the classification methods shows that the vast majority of our observed dSSW events are categorized as PWDs.

3.3 Implications for the upper-tropospheric jet stream

Next, a closer look at the impact of dSSWs and nSSWs on the upper-tropospheric jet stream contributes to the general downward propagation picture. Figure 5 displays two time series of jet latitude anomalies spanning 90 days before and after the central date of dSSWs and nSSWs, respectively. Generally, jet latitude variability is high between individual SSW events (refer to Figs. S4 and S5 in the supplementary material). Nevertheless, the upper-tropospheric jet stream is significantly displaced southward during dSSWs. This displacement occurs almost immediately after the central date, lasts for nearly the entire 50-day

https://doi.org/10.5194/egusphere-2024-667
Preprint. Discussion started: 7 March 2024

period following dSSWs' onset, and reaches composite mean anomalies of up to 1° latitude around lag 25. Some individual dSSW events even exhibit jet latitude anomalies of around and below -2° N after the central date (Fig. S4). At around lag 25, when the composite mean peaks, all but one of the individual dSSW events show an equatorward displacement of the upper-tropospheric jet for a bit longer than ten consecutive days.

In contrast, nSSW events do not demonstrate this equatorward displacement. Although a weaker and shorter equatorward displacement may be suspected also around the central date of nSSWs, the smaller and shorter latitude fluctuations seen in the composite of Fig. 5 are masked by the high variability between individual events (Fig. S5). None of the days within this period of $\pm$ 90 days around the central date of nSSWs shows a significant jet latitude anomaly.

These findings are in line with the observed downward propagation patterns and surface imprints (Figs. 1-4). Specifically, while nSSW events do not display a clear and significant surface signal, dSSW events result in a negative NAM-like situation with a southward displaced upper-tropospheric jet, as anticipated from the classification method.

Previous studies examined the effect of stratospheric events on the lower-tropospheric North Atlantic eddy-driven jet (Maycock et al., 2020; Goss et al., 2021). These studies used a jet latitude index (Woollings et al., 2010) to distinguish three distinct lower-tropospheric jet regimes and found an increased occurrence of the southern jet regime over the North Atlantic in both reanalysis and model data. While these results align with our observed dSSW response, it is important to note that their methodology is different from our global upper-tropospheric approach and does not distinguish between d/nSSWs.

4 Planetary and synoptic-scale wave activity behavior

Finally, the relationship between the downward propagation of the stratospheric SSW signal and planetary to synoptic-scale wave activity is analyzed and discussed.

Previous modeling studies of varying complexity (e.g. Song and Robinson (2004); Butler et al. (2010); Garfinkel et al. (2013); Domeisen et al. (2013); Hitchcock and Simpson (2014); Smith and Scott (2016); White et al. (2020); Rupp and Birner (2021)) have started to shed light on the role of synoptic-scale waves in stratosphere-troposphere coupling during SSWs. First observational evidence was given by Limpasuvan et al. (2004) in their study of the composite life cycle of all SSWs using reanalysis data. Their time-height composites of Eliassen-Palm flux components show significant differences between planetary and synoptic-scale wave numbers and suggest a key contribution of synoptic-scale waves in coupling the stratospheric anomalies to the troposphere. More recent observational hints at increased vertical propagation and activity of synoptic-scale waves prior to SSWs come from Pilch Kedzierski et al. (2020), their studied cases incidentally being dSSWs.

In this section, we can deliver a more general observational confirmation while agreeing with previously suggested mechanisms on stratosphere-troposphere coupling. In addition, the separation into d/nSSWs yields a clearer picture. Latitude-height composites of planetary and synoptic-scale wave activity during dSSWs and nSSWs averaged over different lags around the central date are shown in terms of EKE (Fig. 6), heat fluxes (Fig. 7), and momentum fluxes (Fig. 8).

https://doi.org/10.5194/egusphere-2024-667
Preprint. Discussion started: 7 March 2024

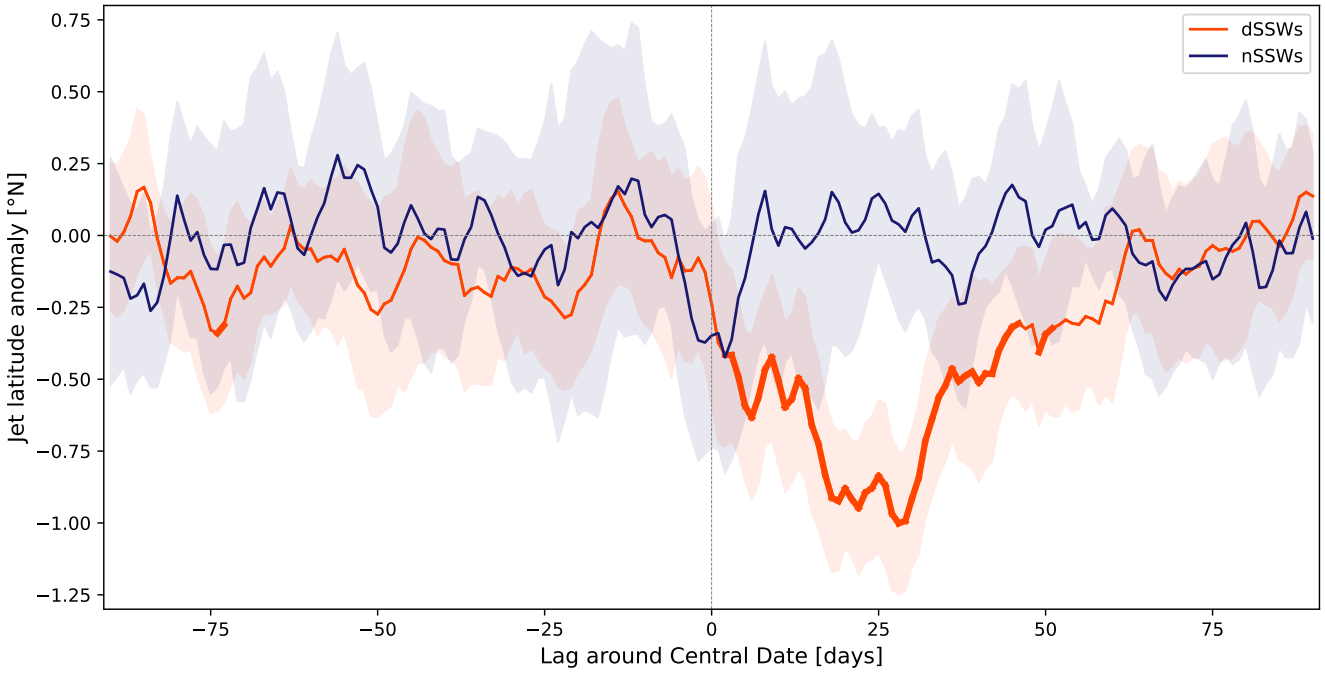

Figure 5. Composites of jet latitude anomalies in °N for different lags around the central date of dSSWs and nSSWs, respectively. Shading indicates the 90 % confidence intervals; a thicker line marks the days with jet latitude anomalies significantly different from the climatology at a 95 % confidence level.

4.1 EKE

Planetary EKE (Fig. 6a-b) is similar preceding the onset of both dSSWs and nSSWs, except for a stronger positive tropospheric signal around 40° N before the central date of nSSWs. Interestingly, however, synoptic-scale EKE anomalies (Fig. 6c-d) in the troposphere are opposite in sign depending on the downward influence: we see strong positive anomalies preceding dSSWs, while EKE is significantly reduced before nSSWs.

After the central date, the tropospheric planetary wave burst that is observed at higher latitudes during the onset stage lasts for dSSWs, whereas nSSWs show significant negative EKE anomalies in this region. In the stratosphere, the zero-wind line is found at a maximum height of around 10 hPa after the central date of dSSWs and is seen to descend over time. In line with the disruption of the polar vortex as seen in the downward propagation patterns in Section 3, planetary wave propagation to the stratosphere is inhibited and, accordingly, seen to be significantly reduced, especially at polar latitudes.

Synoptic-scale EKE (Fig. 6c-d) below the tropopause stays at elevated levels during all lags after dSSWs onset (taking into account the decrease with latitude in tropopause height). Also the lowermost stratosphere at 30 to 45° N shows very persistent significant positive anomalies that are not consistently present during nSSWs. This increased activity of synoptic-scale EKE is in line with the findings of Pilch Kedzierski et al. (2020), who found Rossby wave packet (RWP) activity propagation into the

https://doi.org/10.5194/egusphere-2024-667
Preprint. Discussion started: 7 March 2024

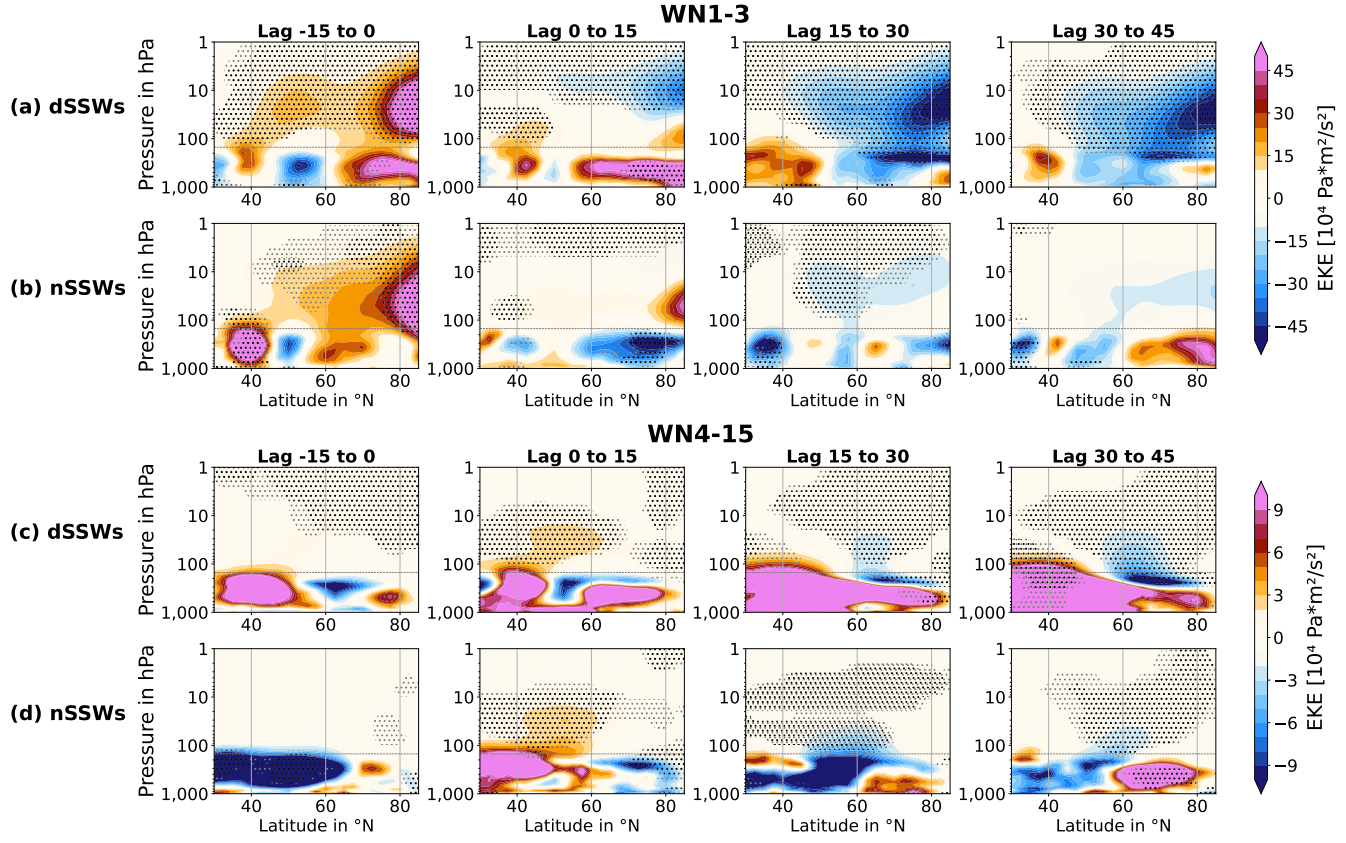

Figure 6. Latitude-height composites of pressure-weighted eddy kinetic energy (EKE) averaged over 15-day periods around the central dates during (a) dSSWs and (b) nSSWs for planetary waves (zonal wave numbers 1 to 3) as well as for synoptic-scale waves (zonal wave numbers 4 to 15) during (c) dSSWs and (d) nSSWs. Black hatching indicates significant differences at a 95 % confidence level, gray hatching at a 90 % confidence level. The thin, gray horizontal line marks the 150 hPa level.

stratosphere to increase markedly in their case study of the SSWs of 2009, 2010, and 2013, which are all classified as dSSWs (compare Table S1). After 30 days after the central date of dSSWs, strong and significant synoptic-scale EKE anomalies reach down to the lowermost troposphere, thereby indicating a coupling between the stratosphere and the surface. During the same lags, synoptic-scale EKE for nSSWs shows a purely tropospheric signal that is even opposite in sign compared to dSSWs at mid-latitudes.

4.2 Heat fluxes

Also for heat fluxes, planetary wave activity (Fig. 7a-b) is increased and very similar preceding the central date of d/nSSWs. In the days before the SSW's onset, both troposphere and stratosphere show elevated levels of planetary heat fluxes over a broad range of latitudes between 45 and 80° N. After the central date of dSSWs, planetary heat fluxes first stay at significantly

https://doi.org/10.5194/egusphere-2024-667
Preprint. Discussion started: 7 March 2024

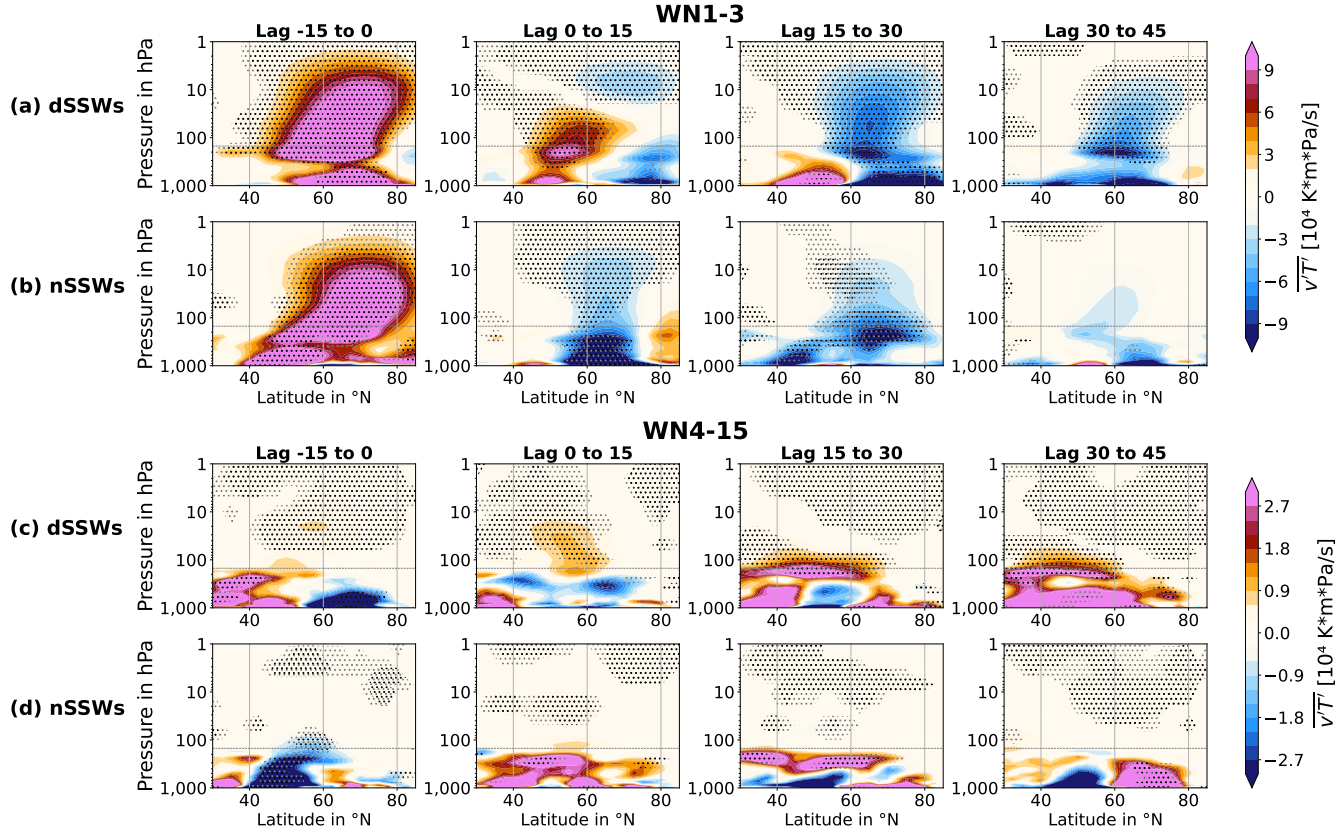

Figure 7. As Fig. 6 but for latitude-height composites of heat fluxes ($\overline{v'T'}$). Again, black (gray) hatching indicates significant differences at a 95 % (90 %) confidence level.

increased values below the zero-wind line before negative anomalies dominate the stratosphere after lag 15, which is in line with the negative planetary EKE anomalies (Fig. 6a-b) and the disruption of the polar vortex (Fig. 3a-c) (compare Charlton and Polvani, 2007; Hitchcock and Simpson, 2014; Karpechko et al., 2017). Planetary heat fluxes following the central date of nSSWs, however, are immediately characterized by significant negative anomalies between 50 and 70° N.

For synoptic-scale heat fluxes (Fig. 7c-d), the troposphere is characterized by significant negative anomalies between 40 and 60° N before the onset of nSSWs, whereas dSSWs are preceded by significantly increased tropospheric heat fluxes between 30 and 50° N. After lag 15 of dSSWs, vertical propagation of synoptic-scale waves is significantly increased in the lower stratosphere. During the same lags after the central date, nSSWs do not show coherent and significant anomalies at these heights. This supports the role of the lower stratosphere in maintaining the stratospheric signal for downward propagation as suggested by Karpechko et al. (2017) and White et al. (2020), see review in Baldwin et al. (2021). It also shows that the surface coupling during dSSWs is through synoptic-scale waves, which has not been confirmed in observational studies before.

https://doi.org/10.5194/egusphere-2024-667
Preprint. Discussion started: 7 March 2024

Both the prolonged planetary heat flux activity after the onset as well as the extended synoptic-scale heat flux burst following dSSW events explain the coincidence with precursors and spatial patterns of 'positive wave driving' (PWD) events identified by Reichler and Jucker (2022): the PWD definition is based on integrated lower-stratospheric heat fluxes, i.e. the region that exhibits increased heat fluxes during dSSWs.

A possible role of the observed EKE and heat flux anomalies for the downward propagation of the SSW signal lies in the interaction across scales between planetary and synoptic-scale waves. Before the onset of dSSW events, synoptic-scale EKE and heat fluxes at mid-latitudes are above average, which is not observed prior to nSSWs. Planetary wave activity, however, is very similar preceding both dSSW and nSSW events. It is conceivable that, instead of (or apart from) directly influencing the mean flow, the synoptic-scale waves interfere with the planetary waves via triad interaction (Boljka and Birner, 2020). By taking energy from the synoptic-scale waves (i.e., upscale cascade as explained by Boljka and Birner (2020)), planetary EKE and heat flux anomalies could persist longer during dSSWs. This could help explain the substantial d/nSSW differences seen in planetary EKE and heat fluxes right after the central date (Figs. 6a-b and 7a-b). We speculate that the mechanism of triad interaction provides a plausible explanation for the observed anomalies in EKE and heat fluxes. This, however, requires further study to confirm and is worth exploring in the future.

4.3 Momentum fluxes

Generally, momentum flux anomalies (Fig. 8) during both dSSWs and nSSWs are seen to be less consistent, also in sign, over different pressure levels and latitudes compared to EKE and heat flux anomalies, and the (pressure-weighted) momentum flux signal is mostly tropospheric.

Planetary momentum fluxes (Fig. 8a-b) show the clearest and most consistent signal after the central date of dSSWs: first significant negative tropospheric anomalies at mid-latitudes right after dSSWs' onset, followed by enhanced poleward momentum fluxes in the troposphere after lag 15 at latitudes around 40° N.

Before the central date, also synoptic-scale momentum fluxes (Fig. 8c-d) do not display a clear and significant signal. Intriguingly, however, the troposphere following dSSWs is characterized by very consistent significant negative anomalies. They indicate a remarkable reduction of the poleward momentum fluxes in the climatological mean, especially at mid-latitudes south of 55° N (compare the mean wintertime composite in Fig. S6 in the supplement). The tropospheric signal following nSSWs is less consistent across latitudes, but features strong positive anomalies south of 50° N, thereby enhancing the mean poleward momentum fluxes in this region.

Garfinkel et al. (2013) found a relationship between tropospheric synoptic-scale eddy momentum fluxes and the response in jet latitude to stratospheric perturbations in a dry primitive equation model. More specifically, they found that stratospheric focused mechanisms alone could not explain the jet latitude response, whereas processes involving the strength of tropospheric synoptic-scale eddy momentum fluxes appeared to be essential for this response.

A role of synoptic-scale momentum fluxes for the downward coupling of the SSW signal was also described in a modeling study by Rupp and Birner (2021). They studied changes in the evolution of idealized baroclinic life cycles induced by the presence of a stratospheric jet, with post-SSWs conditions being represented by a model set-up with only a tropospheric jet.

https://doi.org/10.5194/egusphere-2024-667
Preprint. Discussion started: 7 March 2024

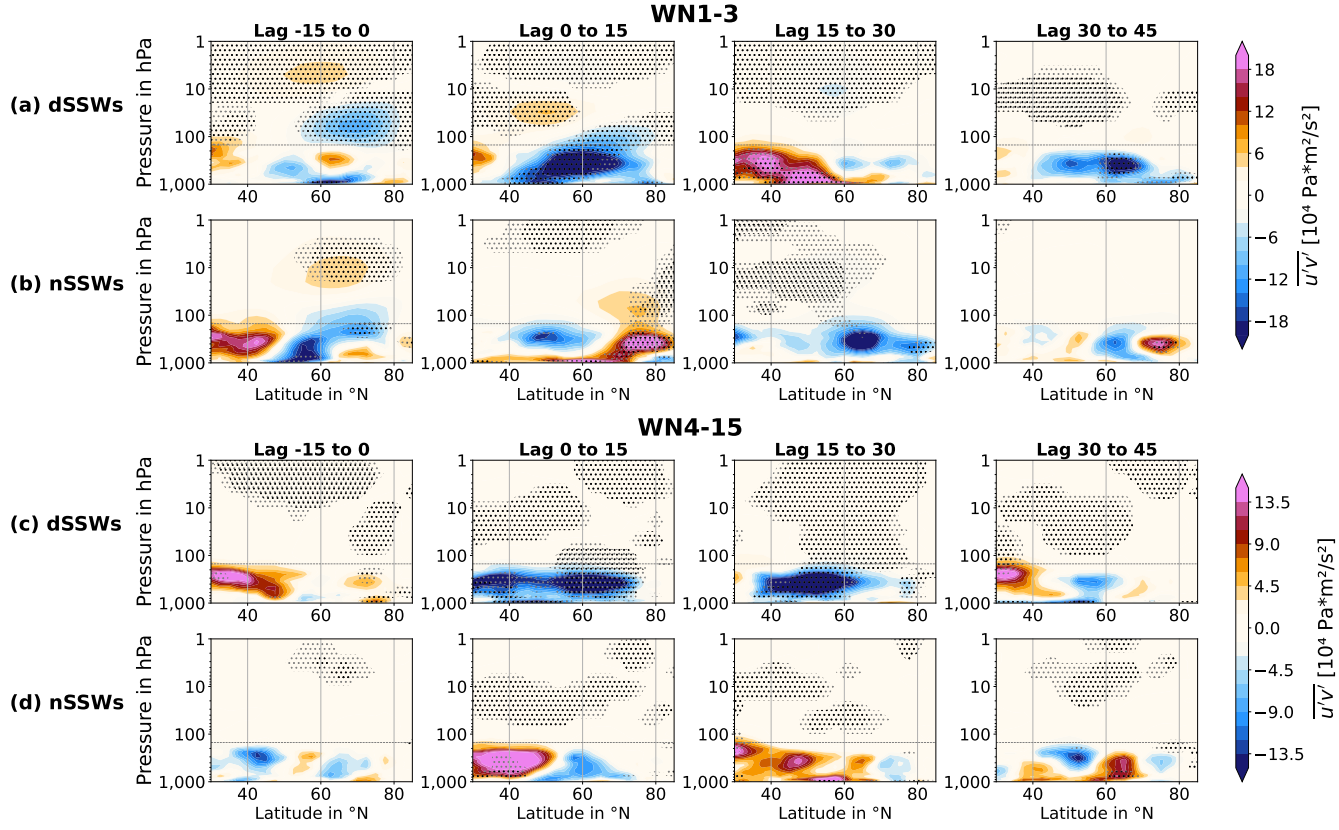

Figure 8. As Figs. 6 and 7 but for latitude-height composites of momentum fluxes ($\overline{u'v'}$). Again, black (gray) hatching indicates significant differences at a 95 % (90 %) confidence level, respectively.

Their findings suggest that the well-known negative NAM-like response to a missing stratospheric jet is accompanied by reduced eddy momentum transport at the tropopause level. This is in line with weaker poleward synoptic-scale momentum fluxes during dSSWs compared to nSSWs in our Fig. 8c-d. From our observational results, the mechanism of reduced momentum fluxes from synoptic-scale waves appears to act more effectively during dSSWs (Fig. 8c-d), which is supported by the observed jet stream equatorward migration (Fig. 5), and hence the stronger coupling to the surface.

For completeness, the daily evolutions of d/nSSW differences averaged over two latitude bands are shown in Figs. S7 and S8 in the supplement, supporting the 15-day averages shown here.

5 Conclusions

This study focuses on identifying downward propagation patterns of SSWs in ERA5 reanalysis data and investigating the behavior of the upper-tropospheric jet stream and planetary and synoptic-scale waves throughout their development.
Our main findings are as follows:

https://doi.org/10.5194/egusphere-2024-667
Preprint. Discussion started: 7 March 2024

1. The observed spatial temperature and geopotential height patterns during dSSWs (Figs. 1 and 3) and nSSWs (Figs. 2 and 4) show a stronger and longer-lasting dSSW signal and support the classification following Karpechko et al. (2017), even for near-surface level regional impacts.

2. Tropospheric precursors for nSSWs are seen in the form of significant warm anomalies over Canada and the Labrador Sea (Fig. 2d-e), while dSSW events are preceded by high pressure anomalies over eastern and northern Europe (Fig. 3d-e).

3. In line with the negative NAM-like response, the upper-tropospheric jet stream is significantly displaced equatorwards following dSSWs but not nSSWs (Fig. 5).

4. The analysis of wave activity shows a remarkable difference in timing for planetary and synoptic-scale EKE and heat flux anomalies (Figs. 6 and 7). Around the central date of dSSWs, stratospheric planetary wave activity is enhanced before progressing to lower levels and, in the case of EKE from synoptic-scale waves, even coupling to the surface after lag 30. This downward-progression and surface coupling is not observed after nSSW events.

5. Synoptic-scale momentum fluxes in the upper troposphere are significantly reduced following dSSWs but not nSSWs (Fig. 8). This aligns well with the equatorward displacement of the upper-tropospheric jet and confirms the importance of tropospheric eddy feedbacks for the surface coupling found previously in modeling studies (e.g. Rupp and Birner, 2021).

The results presented in our study highlight the important role of synoptic-scale waves in coupling the stratospheric SSW signal to the surface. Also, the observed d/nSSW differences for EKE and heat flux activity suggest a potential interaction across scales between planetary and synoptic-scale waves (Boljka and Birner, 2020), although this requires further investigation and a more targeted analysis.

Code and data availability. The ERA5 reanalysis data set used for this study can be downloaded from the Copernicus Climate Data Store: https://doi.org/10.24381/cds.bd0915c6. Python 3.7.3 was used for the analysis and can be found here: https://www.python.org/downloads/release/python-373/.

Author contributions. TR performed the analyses, produced all figures and wrote the paper with substantial support from RPK, who also designed the methodology. MH implemented the jet stream analysis. KM initiated the study and contributed with ideas and feedback in the early stages.

Competing interests. The authors declare that they have no conflict of interest.

https://doi.org/10.5194/egusphere-2024-667
Preprint. Discussion started: 7 March 2024

Acknowledgements. A first version of the results for the spatial downward propagation patterns discussed here was obtained as part of a Bachelor thesis under the supervision of Katja Matthes and Robin Pilch Kedzierski (Rahm, 2019). We thank Alexey Karpechko for the personal communication in the early phase of this work.

https://doi.org/10.5194/egusphere-2024-667
Preprint. Discussion started: 7 March 2024

References

Archer, C. L. and Caldeira, K.: Historical Trends in the Jet Streams, Geophysical Research Letters, 35, https://doi.org/10.1029/2008GL033614, 2008.

Baldwin, M. P. and Dunkerton, T. J.: Stratospheric Harbingers of Anomalous Weather Regimes, Science (New York, N.Y.), 294, 581–584, https://doi.org/10.1126/science.1063315, 2001.

Baldwin, M. P. and Thompson, D. W.: A Critical Comparison of Stratosphere-Troposphere Coupling Indices, Quartely Journal of the Royal Meteorological Society, 135, 1661–1672, https://doi.org/10.1002/qj.479, 2009.

Baldwin, M. P., Ayarzagüena, B., Birner, T., Butchart, N., Butler, A. H., Charlton-Perez, A. J., Domeisen, D. I., Garfinkel, C. I., Garny, H., Gerber, E. P., Hegglin, M. I., Langematz, U., and Pedatella, N. M.: Sudden Stratospheric Warmings, Reviews of Geophysics, 59, e2020RG000 708, https://doi.org/10.1029/2020RG000708, 2021.

Bancalá, S., Krüger, K., and Giorgetta, M.: The Preconditioning of Major Sudden Stratospheric Warmings, Journal of Geophysical Research, 117, D04 101, https://doi.org/10.1029/2011JD016769, 2012.

Barriopedro, D. and Calvo, N.: On the Relationship between ENSO, Stratospheric Sudden Warmings, and Blocking, Journal of Climate, 27, 4704–4720, https://doi.org/10.1175/jcli-d-13-00770.1, 2014.

Boljka, L. and Birner, T.: Tropopause-Level Planetary Wave Source and Its Role in Two-Way Troposphere–Stratosphere Coupling, Weather and Climate Dynamics, 1, 555–575, https://doi.org/10.5194/wcd-1-555-2020, 2020.

Butler, A. H., Thompson, D. W., and Heikes, R.: The Steady-State Atmospheric Circulation Response to Climate Change–like Thermal Forcings in a Simple General Circulation Model, Journal of Climate, 23, 3474–3496, https://doi.org/10.1175/2010jcli3228.1, 2010.

Charlton, A. J. and Polvani, L. M.: A New Look at Stratospheric Sudden Warmings, Part I: Climatology and Modeling Benchmarks, Journal of Climate, 20, 449–469, https://doi.org/10.1175/JCLI3996.1, 2007.

Domeisen, D. I., Sun, L., and Chen, G.: The Role of Synoptic Eddies in the Tropospheric Response to Stratospheric Variability, Geophysical Research Letters, 40, 4933–4937, https://doi.org/10.1002/grl.50943, 2013.

Domeisen, D. I., Grams, C. M., and Papritz, L.: The Role of North Atlantic–European Weather Regimes in the Surface Impact of Sudden Stratospheric Warming Events, Weather and Climate Dynamics, 1, 373–388, https://doi.org/10.5194/wcd-1-373-2020, 2020.

Fragkoulidis, G., Wirth, V., Bossmann, P., and Fink, AH.: Linking Northern Hemisphere Temperature Extremes to Rossby Wave Packets, Quarterly Journal of the Royal Meteorological Society, 144, 553–566, https://doi.org/10.1002/qj.3228, 2018.

Garfinkel, C. I., Waugh, D. W., and Gerber, E. P.: The Effect of Tropospheric Jet Latitude on Coupling between the Stratospheric Polar Vortex and the Troposphere, Journal of Climate, 26, 2077–2095, https://doi.org/10.1175/jcli-d-12-00301.1, 2013.

Goss, M., Lindgren, E. A., Sheshadri, A., and Diffenbaugh, N. S.: The Atlantic Jet Response to Stratospheric Events: A Regime Perspective, Journal of Geophysical Research: Atmospheres, 126, e2020JD033 358, https://doi.org/10.1029/2020JD033358, 2021.

Hall, R. J., Mitchell, D. M., Seviour, W. J. M., and Wright, C. J.: Tracking the Stratosphere-to-Surface Impact of Sudden Stratospheric Warmings, Journal of Geophysical Research: Atmospheres, 126, e2020JD033 881, https://doi.org/10.1029/2020JD033881, 2021.

Haynes, PH., McIntyre, ME., Shepherd, TG., Marks, CJ., and Shine, K. P.: On the "Downward Control" of Extratropical Diabatic Circulations by Eddy-Induced Mean Zonal Forces, Journal of the Atmospheric Sciences, 48, 651–678, https://doi.org/10.1175/1520-0469(1991)048%3C0651:OTCOED%3E2.0.CO;2, 1991.

Hersbach, H., Bell, B., Berrisford, P., Hirahara, S., Horányi, A., Muñoz-Sabater, J., Nicolas, J., Peubey, C., Radu, R., Schepers, D., Simmons, A., Soci, C., Abdalla, S., Abellan, X., Balsamo, G., Bechtold, P., Biavati, G., Bidlot, J., Bonavita, M., De Chiara, G., Dahlgren,

https://doi.org/10.5194/egusphere-2024-667
Preprint. Discussion started: 7 March 2024

P., Dee, D., Diamantakis, M., Dragani, R., Flemming, J., Forbes, R., Fuentes, M., Geer, A., Haimberger, L., Healy, S., Hogan, R. J., Hólm, E., Janisková, M., Keeley, S., Laloyaux, P., Lopez, P., Lupu, C., Radnoti, G., de Rosnay, P., Rozum, I., Vamborg, F., Villaume, S., and Thépaut, J.-N.: The ERA5 Global Reanalysis, Quarterly Journal of the Royal Meteorological Society, 146, 1999–2049, https://doi.org/10.1002/qj.3803, 2020.

Hitchcock, P. and Simpson, I. R.: The Downward Influence of Stratospheric Sudden Warmings, Journal of the Atmospheric Sciences, 71, 3856–3876, https://doi.org/10.1175/jas-d-14-0012.1, 2014.

Karpechko, A. Y., Hitchcock, P., Peters, D. H., and Schneidereit, A.: Predictability of Downward Propagation of Major Sudden Stratospheric Warmings, Quarterly Journal of the Royal Meteorological Society, 143, 1459–1470, https://doi.org/10.1002/qj.3017, 2017.

Kidston, J., Scaife, A. A., Hardiman, S. C., Mitchell, D. M., Butchart, N., Baldwin, M. P., and Gray, L. J.: Stratospheric Influence on Tropospheric Jet Streams, Storm Tracks and Surface Weather, Nature Geoscience, 8, 433–440, https://doi.org/10.1038/ngeo2424, 2015.

Kodera, K., Mukougawa, H., Maury, P., Ueda, M., and Claud, C.: Absorbing and Reflecting Sudden Stratospheric Warming Events and Their Relationship with Tropospheric Circulation, Journal of Geophysical Research: Atmospheres, 121, 80–94, https://doi.org/10.1002/2015jd023359, 2016.

Kolstad, E. W., Breiteig, T., and Scaife, A. A.: The Association between Stratospheric Weak Polar Vortex Events and Cold Air Outbreaks in the Northern Hemisphere, Quarterly Journal of the Royal Meteorological Society, 136, 886–893, https://doi.org/10.1002/qj.620, 2010.

Kretschmer, M., Runge, J., and Coumou, D.: Early Prediction of Extreme Stratospheric Polar Vortex States Based on Causal Precursors, Geophysical Research Letters, 44, 8592–8600, https://doi.org/10.1002/2017gl074696, 2017.

Kunz, T. and Greatbatch, R. J.: On the Northern Annular Mode Surface Signal Associated with Stratospheric Variability, Journal of the Atmospheric Sciences, 70, 2103–2118, https://doi.org/10.1175/JAS-D-12-0158.1, 2013.

Labitzke, K. G. and van Loon, H.: The Stratosphere - Phenomena, History and Relevance, Springer-Verlag Berlin Heidelberg, 1999.

Lehtonen, I. and Karpechko, A. Y.: Observed and Modeled Tropospheric Cold Anomalies Associated with Sudden Stratospheric Warmings, Journal of Geophysical Research: Atmospheres, 121, 1591–1610, https://doi.org/10.1002/2015jd023860, 2016.

Limpasuvan, V., Thompson, D. W. J., and Hartmann, D. L.: The Life Cycle of the Northern Hemisphere Sudden Stratospheric Warmings, Journal of Climate, 17, 2584–2596, https://doi.org/10.1175/1520-0442(2004)017<2584:TLCOTN>2.0.CO;2, 2004.

Lorenz, D. J. and Hartmann, D. L.: Eddy-Zonal Flow Feedback in the Northern Hemisphere Winter, Journal of Climate, 16, 1212–1227, https://doi.org/10.1175/1520-0442(2003)16<1212:effitn>2.0.co;2, 2003.

Maycock, A. C. and Hitchcock, P.: Do Split and Displacement Sudden Stratospheric Warmings Have Different Annular Mode Signatures?, Geophysical Research Letters, 42, 10,943–10,951, https://doi.org/10.1002/2015gl066754, 2015.

Maycock, A. C., Masukwedza, G. I. T., Hitchcock, P., and Simpson, I. R.: A Regime Perspective on the North Atlantic Eddy-Driven Jet Response to Sudden Stratospheric Warmings, Journal of Climate, 33, 3901–3917, https://doi.org/10.1175/JCLI-D-19-0702.1, 2020.

Nakagawa, K. I. and Yamazaki, K.: What Kind of Stratospheric Sudden Warming Propagates to the Troposphere?, Geophysical Research Letters, 33, L04 801, https://doi.org/10.1029/2005gl024784, 2006.

Peings, Y.: Ural Blocking as a Driver of Early-Winter Stratospheric Warmings, Geophysical Research Letters, 46, 5460–5468, https://doi.org/10.1029/2019GL082097, 2019.

Pilch Kedzierski, R., Matthes, K., and Bumke, K.: New Insights into Rossby Wave Packet Properties in the Extratropical UTLS Using GNSS Radio Occultations, Atmospheric Chemistry and Physics, 20, 11 569–11 592, https://doi.org/10.5194/acp-20-11569-2020, 2020.

Rahm, T.: Der Einfluss von plötzlichen Stratosphärenerwärmungen auf die Troposphäre, Bachelor's thesis, Christian-Albrechts-Universität Kiel, 2019.

https://doi.org/10.5194/egusphere-2024-667
Preprint. Discussion started: 7 March 2024

Reichler, T. and Jucker, M.: Stratospheric Wave Driving Events as an Alternative to Sudden Stratospheric Warmings, Weather and Climate Dynamics, 3, 659–677, https://doi.org/10.5194/wcd-3-659-2022, 2022.

Rupp, P. and Birner, T.: Tropospheric Eddy Feedback to Different Stratospheric Conditions in Idealised Baroclinic Life Cycles, Weather and Climate Dynamics, 2, 111–128, https://doi.org/10.5194/wcd-2-111-2021, 2021.

Scaife, AA., Karpechko, A. Y., Baldwin, MP., Brookshaw, A., Butler, AH., Eade, R., Gordon, M., MacLachlan, C., Martin, N., Dunstone, N., et al.: Seasonal Winter Forecasts and the Stratosphere, Atmospheric Science Letters, 17, 51–56, https://doi.org/10.1002/asl.598, 2016.

Scherhag, R.: Die explosionsartigen Stratosphärenerwärmungen des Spätwinters 1951/52, Berichte des Deutschen Wetterdienstes in der US Zone, 6, 51–63, 1952.

Shaw, T. A., Perlwitz, J., and Harnik, N.: Downward Wave Coupling between the Stratosphere and Troposphere: The Importance of Meridional Wave Guiding and Comparison with Zonal-Mean Coupling, Journal of Climate, 23, 6365–6381, https://doi.org/10.1175/2010jcli3804.1, 2010.

Sigmond, M., Scinocca, J. F., Kharin, V. V., and Shepherd, T. G.: Enhanced Seasonal Forecast Skill Following Stratospheric Sudden Warmings, Nature Geoscience, 6, 98–102, https://doi.org/10.1038/ngeo1698, 2013.

Smith, K. L. and Scott, R. K.: The Role of Planetary Waves in the Tropospheric Jet Response to Stratospheric Cooling, Geophysical Research Letters, 43, 2904–2911, https://doi.org/10.1002/2016gl067849, 2016.

Song, Y. and Robinson, W. A.: Dynamical Mechanisms for Stratospheric Influences on the Troposphere, Journal of the Atmospheric Sciences, 61, 1711–1725, https://doi.org/10.1175/1520-0469(2004)061<1711:dmfsio>2.0.co;2, 2004.

Thompson, D. W. J., Baldwin, M. P., and Wallace, J. M.: Stratospheric Connection to Northern Hemisphere Wintertime Weather: Implications for Prediction, Journal of Climate, 15, 1421–1428, https://doi.org/10.1175/1520-0442(2002)015<1421:sctnhw>2.0.co;2, 2002.

Tripathi, O. P., Baldwin, M., Charlton-Perez, A., Charron, M., Eckermann, S. D., Gerber, E., Harrison, R. G., Jackson, D. R., Kim, B.-M., Kuroda, Y., Lang, A., Mahmood, S., Mizuta, R., Roff, G., Sigmond, M., and Son, S.-W.: The Predictability of the Extratropical Stratosphere on Monthly Time-Scales and Its Impact on the Skill of Tropospheric Forecasts, Quarterly Journal of the Royal Meteorological Society, 141, 987–1003, https://doi.org/10.1002/qj.2432, 2015.

White, I. P., Garfinkel, C. I., Gerber, E. P., Jucker, M., Aquila, V., and Oman, L. D.: The Downward Influence of Sudden Stratospheric Warmings: Association with Tropospheric Precursors, Journal of Climate, 32, 85–108, https://doi.org/10.1175/jcli-d-18-0053.1, 2019.

White, I. P., Garfinkel, C. I., Gerber, E. P., Jucker, M., Hitchcock, P., and Rao, J.: The Generic Nature of the Tropospheric Response to Sudden Stratospheric Warmings, Journal of Climate, 33, 5589–5610, https://doi.org/10.1175/jcli-d-19-0697.1, 2020.

Wolf, G. and Wirth, V.: Implications of the Semigeostrophic Nature of Rossby Waves for Rossby Wave Packet Detection, Monthly Weather Review, 143, 26–38, https://doi.org/10.1175/mwr-d-14-00120.1, 2015.

Woollings, T., Hannachi, A., and Hoskins, B.: Variability of the North Atlantic Eddy-Driven Jet Stream, Quarterly Journal of the Royal Meteorological Society, 136, 856–868, https://doi.org/10.1002/qj.625, 2010.